Discovery of polyoxometalate-based HDAC inhibitors with profound anticancer activity in vitro and in vivo

ARTICLE *in* EUROPEAN JOURNAL OF MEDICINAL CHEMISTRY · JUNE 2011

Impact Factor: 3.45 · DOI: 10.1016/j.ejmech.2011.03.036 · Source: PubMed

11 AUTHORS, INCLUDING:

Chenfei Kong
Northeast Normal University
6 PUBLICATIONS **158** CITATIONS
SEE PROFILE

Jun Lu
Northeast Normal University
73 PUBLICATIONS **1,142** CITATIONS
SEE PROFILE

Baiqu Huang
Northeast Normal University
84 PUBLICATIONS **1,287** CITATIONS
SEE PROFILE

Shuxia Liu
Northeast Normal University
61 PUBLICATIONS **1,258** CITATIONS
SEE PROFILE

European Journal of Medicinal Chemistry 46 (2011) 2477–2484

Contents lists available at ScienceDirect

European Journal of Medicinal Chemistry

journal homepage: http://www.elsevier.com/locate/ejmech

Original article

Discovery of polyoxometalate-based HDAC inhibitors with profound anticancer activity *in vitro* and *in vivo*

Zhixiong Dong [a], Ruikang Tan [b], Jian Cao [c], Yang Yang [a], Chenfei Kong [a], Juan Du [a], Shan Zhu [a], Yu Zhang [a], Jun Lu [a], Baiqu Huang [a,*], Shuxia Liu [b,**]

[a] *Institute of Genetics and Cytology, The Key Laboratory of Molecular Epigenetic of Ministry of Education (MOE), Northeast Normal University, Changchun 130024, China*
[b] *The Key Laboratory of Polyoxometalates Science of Ministry of Education (MOE), College of Chemistry, Northeast Normal University, Changchun 130024, China*
[c] *China-Japan Union Hospital of Jilin University, Changchun, China*

ARTICLE INFO

Article history:
Received 10 December 2010
Received in revised form
9 March 2011
Accepted 16 March 2011
Available online 9 April 2011

Keywords:
Polyoxometalate
Histone deacetylase
HDACI
Anticancer effect

ABSTRACT

We obtained 5 positive novel histone deacetylase inhibitors (HDACIs) from a polyoxometalate (POM) library by using a cell-based screening system targeting the *p21* gene promoter. Among them, PAC-320, a new tri-organic-tin-substitute germanotungstate, displayed remarkable extracellular inhibitory activity. Meanwhile, the crystal structure of PAC-320 was characterized by X-ray crystallography. PAC-320 could stably exist under physiological conditions as revealed by UV spectrum, CV and TG. PAC-320 possessed a strong inhibitory effect to intracellular HDAC activity. More significantly, PAC-320 inhibited the growth of a variety of cancer cells, and exhibited remarkable anticancer effect in a hepatocarcinoma H22 cell mice model. This study revealed, for the first time, that the HDAC inhibitory activity is a mechanism by which POMs exert their anticancer effect.

1. Introduction

Histone deacetylases (HDACs) mediate changes in nucleosome conformation and are important in the regulation of gene expression [1]. HDACs are involved in cell-cycle progression and differentiation, and their deregulation is associated with several cancers [2]. HDAC inhibitors, such as Trichostatin A (TSA) and suberoylanilide hydroxamic acid (SAHA), were demonstrated to have antitumor effects [3–5]. HDACIs are a class of promising anticancer drug, because they can trigger cell cycle arrest, induce cell differentiation and/or to promote cell death in cancers, with little toxicity to normal cells.

Since recruitment of HDACs predominantly leads to transcriptional repression of target genes, inhibition of HDAC enzymatic activity reverses this repression and restores the expression of many tumor-suppressor genes, for instance, the cyclin-dependent kinase inhibitor 1A (CDKN1A, *p21*). P21 is a well-characterized tumor suppressor, which negatively modulates cell cycle by inhibiting the activity of cyclin/cdk2 complexes and blocks DNA replication by binding to the proliferating cell nuclear antigen (PCNA) [6,7]. The promoter of *p21* gene contains several binding sites for transcriptional factors Sp1 and Sp3 [8,9], which can recruit co-repressors (e.g., HDAC1, 2, 3, 4 and 6) to inhibit the transcription of *p21* gene [10–14]. A number of studies indicated that the competence of HDACIs to activate the *p21* promoter and to increase p21 protein level was associated with the enhancement of acetylation of the histones H3 and H4 around the gene promoter region [11,12,14–16].

Currently, several small synthetic molecules and natural products of HDACIs have been advanced into clinical trials [17–19]. Among them, SAHA, a hydroxamate compound, has recently been approved for the treatment of cutaneous T-cell lymphoma, thus providing clinical validation of this therapeutic strategy [20]. On the other hand, many of the compounds in clinical development appear to have limitations, including low potency, undesirable safety profiles such as cardiovascular concerns and potential drug–drug interactions via cytochrome P450 inhibition [17,18]. Hence, there remains a significant clinical opportunity for the discovery of effective and specific HDACIs that are safe and well tolerated. Currently, much of the efforts for exploring new HDACIs have been

Abbreviation: HDAC, histone deacetylase; HAT, histone acetylase; HDACI, histone deacetylase inhibitor; POM, polyoxometalate; CV, Cyclic voltammetry; MTT, 3-(4,5-dimethylthiazol-2-yl)-2,5-diphenyltetrazolium bromide; TSA, Trichostatin A; SAHA, suberoylanilide hydroxamic acid; NaB, sodium butyrate; HTS, high throughput screening; CTX, cyclophosphamide; Bu, butyl; Ot, terminal oxygen; Ob, corner-shared oxygen; Oc, edge-shared oxygen atom; TG, Thermogravimatric.

* Corresponding author. Tel.: +86 431 85099798; fax: +86 431 85099768.
** Corresponding author. Tel./fax: +86 431 85099328.
E-mail addresses: huangbq705@nenu.edu.cn (B. Huang), liusx@nenu.edu.cn (S. Liu).

0223-5234/$ – see front matter © 2011 Elsevier Masson SAS. All rights reserved.
doi:10.1016/j.ejmech.2011.03.036

focusing on the screening from numerous organic compounds or modification of existing HDACI compounds, while the inorganic HDACIs have not been reported so far.

Polyoxometalates (POMs), as early transition-metal oxide clusters, possess extremely rich diversity in composition, structure and electronic properties, all which make them valuable in applications such as optics, electricity, magnetics, materials, catalysis and medicine [21–23]. An attractive feature of polyoxometalates is that rational and reproducible synthetic methods are now available for the replacement of one or more of the skeletal d0 early transition-metal cations in POMs with d- or p-block ions, and also for the covalent attachment of organic groups to POMs via linkages that are compatible with physiological conditions. Both metal substitution and organic derivatization extend considerably the number of POMs that are potentially available. Pendent organic/biological groups can be used to modulate bioavailability, increase recognition of key substructures in target biomacromolecules, and enhance the facility of drug formulation [24]. Therefore, study of polyoxometalates as medicinal chemistry has been a focus of research attention [25–27]. Recently, a number of polyoxometalates, such as PM-17, PM-26, PM-32, and organotitanium-substituted heteropolytungstates α-$K_4H_3[(CpTi)_3GeW_9O_{37}]\cdot 10H_2O$, were also found to exhibit antitumor activities in various cancers *in vitro* and/or *in vivo* [28–31]. It was shown that the formation of the 1:1 $[Mo_7O_{24}]^{6-}$-FMN complex in tumor cell mitochondria inhibited ATP generation with a resultant antitumor activity [32]. In addition, Prudent et al. reported that $[P_2Mo_{18}O_{62}]^{6-}$ could inhibit protein kinase CK2 [33], and Müller et al. found that $K_6H_2[TiW_{11}CoO_{40}]$ was a NTPDase inhibitors [34], indicating that POMs may interact with particular proteins, although the molecular mechanisms underlying their anticancer functions have not been extensively investigated.

In this study, we constructed a screening system for high throughput screening (HTS) of HDACIs, in an attempt to identify novel HDACIs from a polyoxometalate library. We discovered 5 compounds that had HDAC inhibitory activity, among which, PAC-320, a new tri-organic-tin-substitute germanotungstate, possessed remarkable HDAC inhibitory activity. Meanwhile, PAC-320 exhibited significant anticancer effect *in vitro* and *in vivo*. These results suggested that suppression of the growth of tumor cells through inhibiting HDAC activity may be an anticancer mechanism of some POMs. This provides important insights into the anticancer mechanisms of POMs.

2. Chemistry

In this article, we describe the preparation of a new polyoxometalate compound PAC-320, according to the general procedure detailed in Experimental Protocols. Meanwhile, crystal structure of PAC-320 was characterized by X-ray crystallography and stability studies of PAC-320 were carried out by using UV spectrum, CV and TG.

3. Pharmacology

We investigated the cytotoxic effects of the new HDACI, PAC-320, screened from a POM library, in six different carcinoma cell lines, i.e., human lung cancer cells (A549), human colon carcinoma cells (SW620), human hepatocellular carcinoma (HepG2), human breast cancer cells (MM-231), human gastric adenocarcinoma (MGC-803), and mouse hepatocarcinoma cells H22, as well as a human normal hepatocellular cell L-02, using the standard MTT assays. Also, the antitumor activity of PAC-320 *in vivo* was further studied in a hepatocarcinoma H22 mice model.

4. Results and discussion

4.1. Screening

High throughput screening for deacetylase inhibition was reported previously [35–38]; however, the screening system used was not cell-based and the procedure was relatively expensive. One of the purposes of this study was to establish a more efficient cell-based system and to screen novel potential HDACIs from a polyoxometalate (POM) library. A stably transfected human embryonic kidney 293 cell line with the plasmid of luciferase reporter gene driven by the *p21* gene promoter was established (for details, see "Experimental Protocols"). To perform the screening, cells were treated with diverse types of POM compounds at different concentrations, and the luciferase reporter activity was determined by using the Squal-luciferase reporter assay system provided by Promega. HDACIs may activate the *p21* promoter, which in turn drives the expression of luciferase gene located downstream of the promoter, resulting in an enhanced luciferase activity. We assayed a total of about 400 polyoxometalate compounds using this cell-based screening system, and 34 compounds were found to be able to increase the luciferase activity, to a variable extent (Table 1 and Table S1). Among them, 5 compounds, which fall into 4 classes, were able to increase the reporter activity by more than 2 folds in contrast to the untreated controls, and this potentiality was similar to that of the positive controls of Trichostatin A (TSA) and sodium butyrate (NaB), the 2 widely used HDACIs (Table 1). These 5 compounds were then used in the following experiments. As shown in Fig. 1, they were able to enhance reporter activity in a reproducible and dose-dependent

Table 1
The luciferase induction values of the 5 potential polyoxometalate HDACIs (TSA and NaB were the positive controls).

Compounds	Code names	Luciferase induction values		
Negative control		541.7		
Positive controls				
Trichostatin A	TSA	1892 (50 ng/mL)		
Sodium butyrate	NaB	2413 (400 μg/mL)		
Drugs		10(μg/mL)	100(μg/mL)	400(μg/mL)
The Keggin-sandwich type of germanotungstates				
$K_8Na_{14}[Co_4(H_2O)_2(GeW_9O_{34})_2]\cdot 25H_2O$ [39]	PAC-304	726.5	1974	2243
$K_4Co_2(H_2O)_{12}[Co_4(H_2O)_2(GeW_9O_{34})_2Co_2(H_2O)_{10}]\cdot 17H_2O$ [40]	PAC-317	686.4	1863	2168
Trimeric tri-Ti(IV)-substituted Keggin-type germanotungstate				
$H_{12}K_{10}[(GeO_3)(OH)(GeW_9Ti_3O_{38})_3]\cdot 18H_2O$ [41]	PAC-334	386.6	1139	1840
Tri-organic-tin-subsititude Dawson-type phosphotungstate				
$K_{6.5}H_{2.5}[(BuSn)_3P_2W_{15}O_{59}]\cdot 15H_2O$ [42]	PAC-128	584.6	1248	1789
Tri-organic-tin-subsititude Keggin-type germanotungstate				
$\{(n\text{-}Bu)Sn(OH)\}_3GeW_9O_{34}]^{4-}\cdot 26H_2O$	PAC-320	1357	2044	1852

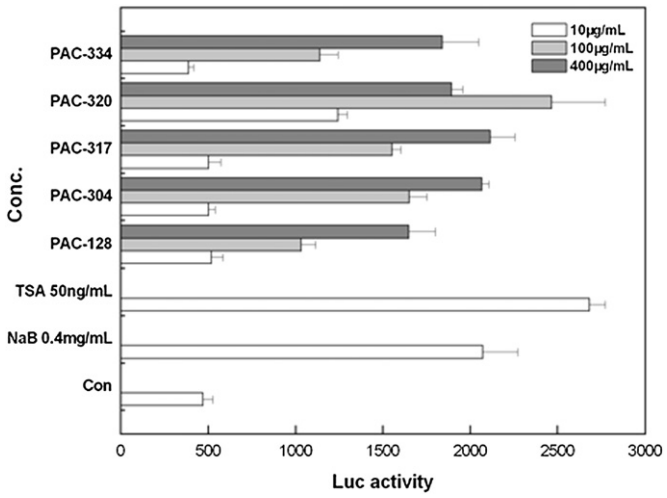

Fig. 1. The 5 positive polyoxometalate compounds upregulated the *p21* promoter reporter gene activity at a dose-dependent manner. TSA and NaB were the positive controls.

manner. Among the 5 compounds, PAC-320, a new tri-organic-tin-substitute germanotungstate compound, exhibited a comparable effect with other compounds but at a lower concentration of 100 μg/mL (Fig. 1). The structural formula and codes of the 5 compounds are shown in Table 1 and Fig. 2.

Additionally, we assayed PM-8, a previously identified anti-tumor polyoxometalate [28,29,43], and found that it failed to significantly increase the luciferase activity (data not shown), suggesting that its antitumor effect was not attributable to HDACI activity.

4.2. Identification of HDAC inhibitory activity

To define the HDACI nature of these polyoxometalates, we evaluated the abilities of the compounds to inhibit HDAC activity by measuring the substrate HDAC fluorescence intensity using an HDAC assay kit (BIOMOL International, Inc.) according to manufacturer's instruction. Synthetic HDAC substrates were added to HeLa cell lysates containing HDACs in the presence or absence of candidate polyoxometalate HDACIs, and the developer was added after a 30-min reaction. Deacetylation of the substrate sensitizes it to the developer, which then generates a fluorophore. The fluorophore was excited with 360 nm light and the emitted light (460 nm) was

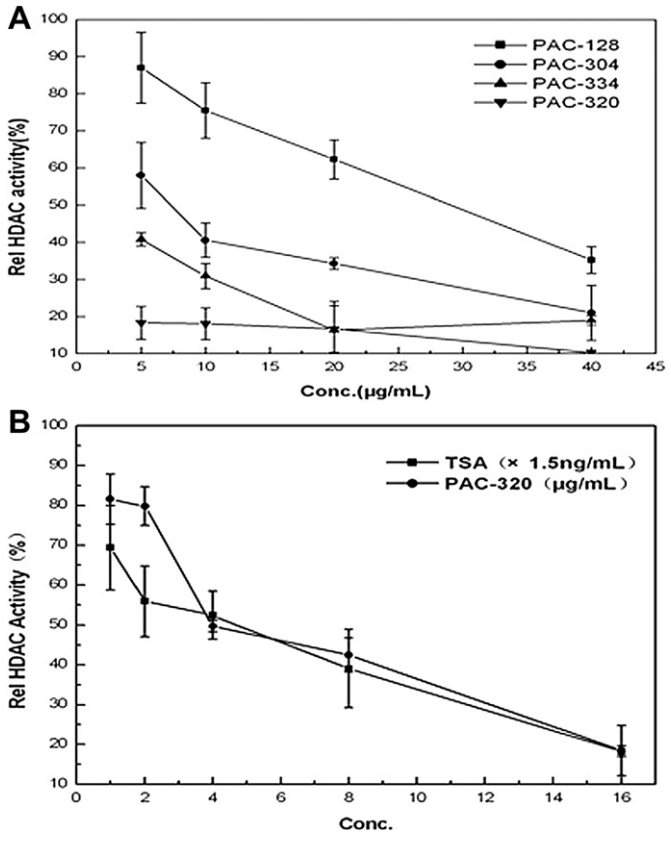

Fig. 3. Histone deacetylase (HDAC)-inhibitory activity of polyoxometalate HDACIs. (A) *In vitro* HDAC inhibition assay. Results are shown as the mean based on experiments performed in triplicate; bars, ±SD. (B) Comparison of the HDAC inhibitory activities between PAC-320 and TSA.

detected on a fluorometric plate reader. As can be seen in Fig. 3A, PAC-128, PAC-304, PAC-334 and PAC-320 displayed the HDACI activities, to a variable extent, in a concentration-dependent manner. Among them, PAC-320 was shown to possess higher inhibitory activity at a relatively low concentration, and this consisted with the above results (Fig. 1). To compare the HDAC inhibitory potency of these POMs, we calculated the IC_{50} values of these compounds in molar concentration (Table S2). It is clear from the table that the compound PAC-334 had a similar IC_{50} value to that of PAC-320. However, in our screening experiments, we found that PAC-334 had a higher toxicity than PAC-320, as the HEK293 cells

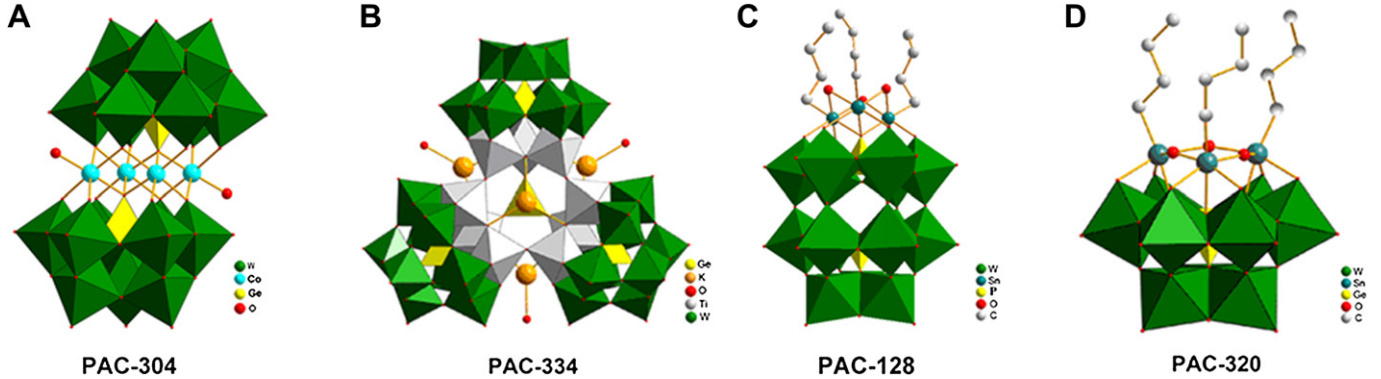

Fig. 2. Combined polyhedral/ball-and-stick representation of polyanions. (A) $[Co_4(H_2O)_2(GeW_9O_{34})_2]^{12-}$ (PAC-304), (B) $[(GeO_3)(OH)(GeW_9Ti_3O_{38})_3]^{22-}$ (PAC-334), (C) $[(BuSn)_3P_2W_{15}O_{59}]^{9-}$ (PAC-128), and (D) $[\{(n\text{-}Bu)Sn(OH)\}_3GeW_9O_{34}]^{4-}$ (PAC-320).

exhibited necrosis phenotype after PAC-334 treatment (data not shown). Further more, the extracellular HDAC inhibitory activity of PAC-320 was compared with TSA, and the results suggested that PAC-320 could inhibit the HDAC activity in a dose-dependent manner comparable to TSA (Fig. 3B). These data suggested that PAC-320 is the most promising HDACI as a potential anticancer agent among polyoxometalates screened.

The POM compounds had HDACI activity belong to 4 different classes. As depicted in Fig. 2, the compounds PAC-304, PAC-317, PAC-334 and PAC-320 contain a common $[A\text{-}\alpha\text{-}GeW_9O_{34}]^{10-}$ fragment, exhibiting the monomeric (PAC-320), dimeric (PAC-304 and PAC-317) or trimeric (PAC-334) polyanions structures, and both the PAC-128 and PAC-320 had $[n\text{-}BuSn]^{3+}$ groups, exhibiting the monomeric polyanions structures. Among them, PAC-320 possesses not only the $[A\text{-}\alpha\text{-}GeW_9O_{34}]^{10-}$ fragment but also $[n\text{-}BuSn]^{3+}$ groups. As can be seen in Figs. 1 and 3, PAC-320 possessed the high potent in upregulating the luciferase reporter activity and in inhibiting extracellular HDAC activity among the POM HDACIs screened. Whether this superior potential in inhibiting HDACs is due to its structural particularity demands a more detailed investigation.

We next sought to determine the intracellular HDAC inhibitory and anticancer activities of the POMs *in vitro* and *in vivo* and PAC-320 was choose as a representative compound for this study.

4.3. Stability studies

To investigate the influences of stability of pH values and time on the compound in aqueous solution, *in situ* UV spectroscopic and cyclic voltammetry measurements of PAC-320 were performed. UV spectrum of PAC-320 in aqueous solution displayed 2 absorption bands centered at about 205 and 259 nm (Fig. 4). The absorption band at 205 nm was attributed to the charge transfer of O_t—W, and the spectral band at 259 nm was assigned to that of O_b/O_c—W [31]. As shown in Fig. 4, the UV spectrum of PAC-320 in aqueous solution displayed 2 absorption bands at about 205 and 259 nm at pH = 4–10. When the pH value gradually decreased to 3, the absorption band at 205 nm disappeared; meanwhile, the characteristic peak at 259 nm decreased slightly (Fig. S2). When the pH value increased to 11 by degrees, with the disappearing of the absorption peak at 205 nm, the spectral band at 259 nm also vanished (Fig. S3). Moreover, the UV spectroscopic of PAC-320 aqueous solution from day 1 to day 30 was also performed at pH = 4–10, and all of the spectra displayed 2 similar absorption peaks at 205 and 259 nm, without obvious change within one month (Fig. S4). The results indicated that the aqueous solution of PAC-320 could stably exist at pH = 4–10 and the stabilization of this aqueous solution could maintain for at least 1 month at ambient temperature.

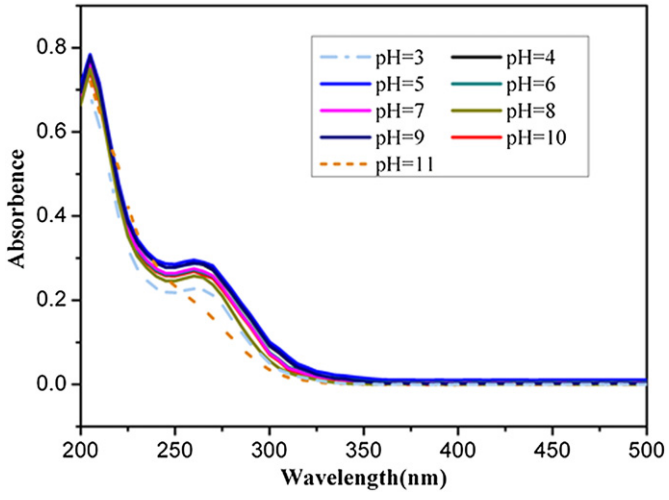

Fig. 4. The UV spectral evolution of PAC-320 in pH = 3–11. The pH was adjusted in the range of 3–7 by addition of aqueous HCl, and in 7–11 by addition of aqueous KOH.

Cyclic voltammetry measurement of PAC-320 was performed in 0.5 M KCl aqueous solution in the potential range of +200 to −1200 mV (scan rate: 100 mV s^{-1}, Fig. S5). The pattern was restricted to the 2 waves, with midpoint potentials (E_{mid}) of −778 (I–I′) and −940 (II–II′) mV, where $E_{mid} = (E_{pc} + E_{pa})/2$; E_{pc} and E_{pa} are the cathodic and anodic peak-potentials, respectively. The redox peaks I–I′ and II–II′ should be ascribed to the redox processes of W (VI) centers [44]. No prominent electrochemical signature for Sn(IV) center was found under the testing conditions. As depicted in Fig. S6, the CV curves slightly changed when the pH values varied in the range of 4–10, indicating that the anion framework of PAC-320 was still retained. However, when the pH values were lower than 3 or higher than 10, the CV curves changed significantly (Fig. S7 and S8), suggesting that the polyoxoanion framework had been decomposed. The *in situ* CV curves of PAC-320 further confirmed that the aqueous solution of PAC-320 could stably existed at pH = 4–10. These results suggested that PAC-320 could stably exist under the physiological conditions.

Furthermore, thermal stability investigation of PAC-320 was carried out and the results also supported its chemical composition. The TG curve of PAC-320 exhibited a total weight loss of 18.95% in the range of 20–600 °C, which was in agreement with the calculated value of 18.74% (Fig. S9). The weight loss of 13.83% at 25–185 °C corresponded to the loss of twenty-six lattice water molecules (calc.13.76%). The weight loss of 5.12% at 185–435 °C was due to the removal of 3 butyl groups (calc.4.98%). These results indicated that the polyoxoanion framework could stably exist below 185 °C.

4.4. Intracellular HDAC inhibit activity assay

We next intended to further verify the intracellular HDAC inhibitory activity of the potential HDACIs in cancer cells, using PAC-320 as a representative compound. We performed immunoblotting to determine its effect on the intracellular levels of acetylated histone H3. H22 mouse hepatocarcinoma cells were treated with various doses of PAC-320, and total protein extracted from the cells was then subjected to sodium dodecyl sulfate polyacrylamide gel electrophoresis (SDS-PAGE) and immunoblotting analysis using specific antibody against acetylated H3. H22 cell line exhibits low basal level of acetylated H3, and we found that PAC-320 induced the hyperacetylation of histone H3 in a dose-dependent manner (Fig. 5). The *in vivo* effect of PAC-320 on nucleosomal histone acetylation correlated well with its cell-free *in vitro* effect on HDAC activity (compare Fig. 3B with Fig. 5). Thus, we obtained a class of novel HDACIs by screening from a polyoxometalate library using a reporter gene system, and we validated that these compounds could inhibit HDAC activity effectively *in vitro* and *in vivo*.

4.5. Cytotoxicity effect

HDACIs have been implicated to have potent antitumor competence in cancer cells [4,45–47]. We then examined the effects of PAC-320 on the growth and proliferation of various cancer cells by using the MTT assay. As shown in Fig. 6A, growth of mouse hepatocarcinoma H22 cells was markedly suppressed in the presence of PAC-320 in a dose-dependent manner. In addition, PAC-320 could restrain the growth of a variety of human cancer cells, including colon carcinoma cells (SW620), gastric adenocarcinoma (MGC-803), lung cancer cells (A549), breast cancer cells (MM-231) and hepatocellular carcinoma (HepG2) (Fig. 6B). Moreover, our results showed

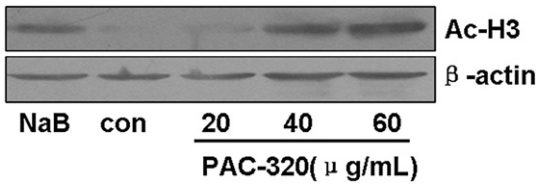

Fig. 5. PAC-320 upregulated the acetylation level of histone H3 in H22 mouse hepatocarcinoma cells in a dose-dependent manner. Amounts of immunoblotted proteins were quantified by normalizing to β-actin.

Table 2
The IC_{50} values of different HDACIs on cancer cell HepG2 and normal cell L-02.

Drugs	HepG2(IC_{50})	L-02(IC_{50})
PAC-320	19.2 ± 5.2 μg/mL	42.8 ± 8.2 μg/mL
SAHA	343.2 ± 65.4 ng/mL	1214.4 ± 237.6 ng/mL
NaB	627 ± 132 μg/mL	528 ± 143 μg/mL

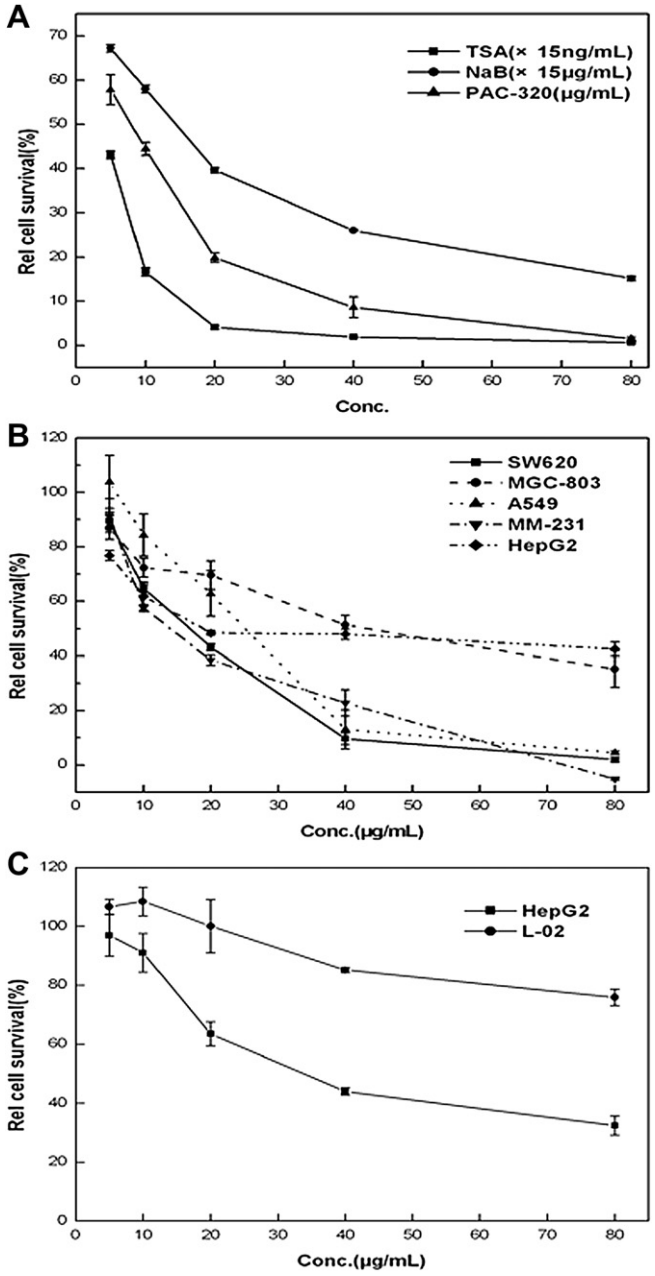

Fig. 6. PAC-320 displayed prominent antiproliferation effects on cancer cells, but had a low toxicity on normal cells. The influences of PAC-320 on the proliferation of mouse hepatocarcinoma cell H22 (A) and on various human cancer cell lines (B) were determined by using the 3-(4,5-dimethylthiazol-2-yl)-2,5-diphenyltetrazolium bromide (MTT) assay. (C) MTT assay determination of the effect of PAC-320 on human hepatocellular carcinoma cell HepG2 and on normal hepatocellular cell L-02. Values represent the mean of 3 experiments; bars, ±SD.

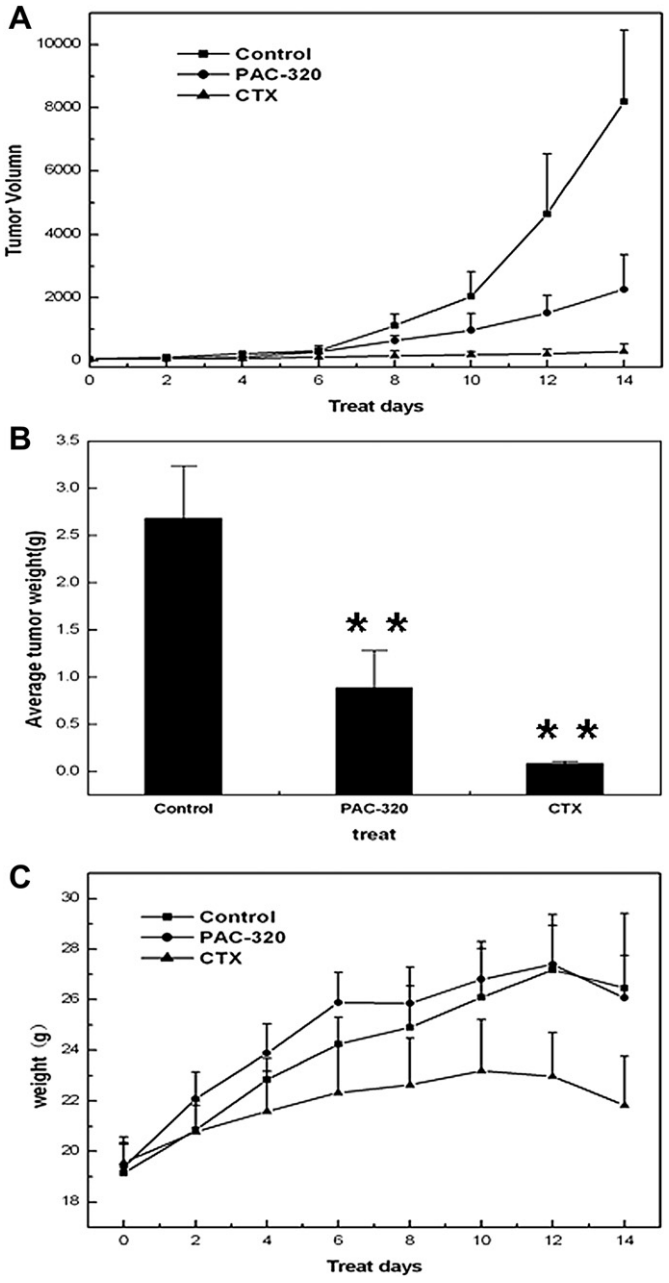

Fig. 7. The antitumor effect of PAC-320 in a hepatocarcinoma cell H22 mice model. (A) Effect of PAC-320 at a dose of 300 mg/kg (determined previously as the maximum tolerated dose), and cyclophosphamide (CTX) at 20 mg/kg on tumor growth. The size of tumor was examined as described in "Experimental Protocols". Drugs were administered intraperitoneally daily into mice bearing tumors for 14 days. Each group contained 6 mice; bars, ±SD. (B) Effects of PAC-320 on tumor weights. Tumor weights were examined upon autopsy. The average weight difference was significant between the two groups (**P, $P < 0.01$). (C) Effects of PAC-320 on mice weight. Mice weight was examined every other day, bars, ±SD.

that PAC-320 was effective in various cancer cell lines with IC_{50} values at the micromolar levels (data not shown). These data clearly indicated that the polyoxometalate compound PAC-320 had potent antiproliferation effect in cancer cells *in vitro*. Meanwhile, MTT assay was also used to compare the toxicity of PAC-320 on tumor and normal cells. As shown in Fig. 6C, PAC-320 had a significant antiproliferation effect on human hepatocellular carcinoma cell HepG2, while it had a minor toxicity on normal hepatocellular cell L-02, and the IC_{50} in tumor cell was much lower than that in normal cell (Table 2). Meanwhile, the toxicity of PAC-320 was tested in comparison with the positive controls SAHA and NaB, and the results revealed that the toxicity of PAC-320 in normal cells was similar to that of SAHA, while it was lower than that of NaB (Table 2). These data suggested that PAC-320 may potentially be a promising antitumor drug.

4.6. Antitumor activity in vivo

To further evaluate the antitumor effect of PAC-320 *in vivo*, we performed an animal study using a hepatocarcinoma H22 mice model. The results demonstrated that the growth of tumors in mice treated with PAC-320 (300 mg/kg) was prohibited by 62.5% compared with that in control mice treated with only diluent (saline) at day 14 (Fig. 7A). The weight of tumor was also significantly reduced in mice treated with PAC-320 (Fig. 7B). By comparison, the antitumor drug cyclophosphamide (CTX) reduced the growth of tumors by 95.5% at day 14 in the same animal system (Fig. 7A); however, CTX also inhibited the growth of mice, implicating its side-effects on normal growth and development of mice (Fig. 7C). Meanwhile, we did not observe significant growth inhibition of mice in the group of PAC-320 treatment (Fig. 7C). These results indicated that PAC-320 had a significant *in vivo* antitumor activity in mice, with little effect on the normal growth of the animals.

5. Conclusions

The *p21* promoter reporter gene screen system used in this study has been proven valuable for screening anticancer HDACIs compounds. We have succeeded in screening novel polyoxometalate HDACIs by utilizing this cell-based *p21* promoter reporter assay system. All the compounds screened were found to possess extracellular inhibitory activity to HDACs. Meanwhile, PAC-320, a new tri-organic-tin-substitute germanotungstate, showed a more effective inhibitory activity. We further confirmed that PAC-320 exhibited remarkable intracellular HDAC inhibitory activity, as well as anticancer competency both *in vitro* and *in vivo* with little harm to the normal growth of the cells and animals.

By analyzing the structure–activity relationships of the POMs screened, we hypothesized that the $[A\text{-}\alpha\text{-}GeW_9O_{34}]^{10-}$ fragment and the $[n\text{-}BuSn]^{3+}$ groups may contribute to the HDAC inhibit activity of POMs. This may be a useful clue for the designing and synthesis of novel polyoxometalate-HDAC inhibitors in the future.

The POM compound PAC-320 identified in this study exhibited many merits, including simple and easy synthesis procedure, high yield, good water solubility and stability under the physiological conditions. These advantages allow for further investigation of the biological activity of PAC-320 for potential cancer chemotherapeutics.

In addition, this study revealed, for the first time, that the HDAC inhibitory activity is one of the mechanisms by which polyoxometalates exhibit their anticancer effect. Clearly, a good understanding of the anticancer mechanisms of polyoxometalates may help to design and modify these compounds for more powerful anticancer agents. Identification of the active products by crystallization of polyoxometalate-HDAC complexes is underway.

6. Experimental protocols

6.1. Chemistry

All the chemicals were obtained commercially and used without additional purification. The lacunary POM precursor $K_8Na_2[A\text{-}\alpha\text{-}GeW_9O_{34}]\cdot 25H_2O$ was synthesized according to the procedure described in the literature [48] and the purity was determined by IR spectra. The polyoxometalates in screening were synthesized according to procedures published by our laboratory (including PAC-304, PAC-334, etc) and published elsewhere (details were described in Support Information). These compounds were confirmed by elemental analysis, Fourier transform IR (FTIR) spectroscopy, UV spectroscopy and NMR spectra.

The IR spectra in KBr pellets were recorded in the range 400–4000 cm^{-1} with an Alpha Centaurt FT/IR Spectrophotometer. Elemental Analysis (C, H) were performed with a Perkin–Elmer 2400 CHN Elemental Analyzer. K, Ge, Sn and W were determined with a PLASMASPEC (I) ICP atomic emission spectrometer. Thermogravimetric analysis was carried out by using a Perkin–Elmer TGA7 instrument, with a heating rate of 10 °C/min, in a nitrogen atmosphere. UV absorption spectra were obtained by using a 752 PC UV spectrophotometer. Electrochemical measurements were performed with CHI660B electrochemical workstation (Chenhua Instruments Co., Shanghai, China). Three-electrode system was employed in this study. The glass carbon electrode ($d = 3$ mm) was used as a working electrode, the Ag/AgCl electrode as a reference electrode and Pt coil as a counter electrode. All potentials were measured and reported versus the Ag/AgCl. All the experiments were conducted at ambient temperature (25–30 °C).

6.1.1. Synthesis of $K_3H[\{(n\text{-}Bu)Sn(OH)\}_3GeW_9O_{34}]\cdot 26H_2O$ (PAC-320)

2.8 g (1 mmol) of powdered $K_8Na_2[A\text{-}\alpha\text{-}GeW_9O_{34}]\cdot 25H_2O$ was quickly added to a solution of 0.6 mL of n-$BuSnCl_3$ (3 mmol) in 50 mL of water at room temperature. After 10 min of vigorous stirring, any undissolved white residue was filtered off. Next, 5.0 g (67 mmol) of solid potassium chloride was added to the filtrate. After stirring for about 1 h, the white precipitate was collected by filtration and air dried [yield 2.7 g (92.0%, based on W)]. Well-formed sheet colorless crystals suitable for X-ray crystallography were obtained by recrystallizing from warm water after 1 week (yield: 95.8%). IR (KBr disks): 2954 (vw), 2924 (vw), 2865 (w), 1460 (m), 1380 (w), 1250 (m), 1181 (w), 1154 (vw), 1100 (s), 952 (vs), 882 (s), 796 (s), 690 (m), 529 (w), 456 (m). Elemental anal. Calcd for $H_{83}C_{12}K_3GeW_9Sn_3O_{63}$: H, 2.42; C, 4.19; K, 3.41, Ge, 2.11; Sn, 10.36; W, 48.15. Found (%): H, 2.39; C, 4.24; K, 3.33; Ge, 2.07; Sn, 10.45; W, 48.28.

6.1.2. X-ray structure analysis

Single-crystal diffractometry was conducted on a Bruker Smart Apex CCD diffractometer with Mo Kα monochromated radiation ($\lambda = 0.71073$ Å) at room temperature. The linear absorption coefficients, scattering factors for the atoms, and the anomalous dispersion corrections were taken from International Tables for X-ray Crystallography. Empirical absorption corrections were applied. The structure was solved by the direct method and refined by the full-matrix least-squares method on F2 using the SHELXS-97. Anisotropic thermal parameters were used to refine all non-hydrogen atoms except for the part of oxygen. Those hydrogen atoms attached to lattice water molecules were not located. The crystal data and structure refinement results of PAC-320 are summarized in Table S3. Bond lengths (Å) and bond angles (°) for PAC-320 is provided in Tables S4. Further details on the crystal structure investigations may be obtained from the Fachinformationszentrum Karlsruhe, 76344 Eggenstein–Leopoldshafen, Germany (fax: +49 7247 808 666; e-mail: crysdata@fiz-karlsruhe.de), on quoting the depository numbers CCDC-779112.

6.2. Biology

6.2.1. Experimental materials, methods and instrumentation

Human embryonic kidney 293 cells (HEK293), Human normal hepatocellular cell L-02, human lung cancer cells (A549), human colon carcinoma cells (SW620), human hepatocellular carcinoma (HepG2), human breast cancer cells (MM-231) and human gastric adenocarcinoma (MGC-803) were obtained from The Shanghai Cell Line Bank, Chinese Academy of Sciences. Cells were grown in IMDM medium supplemented with 10% fetal bovine serum, 100 mg/mL penicillin and 100 mg/mL streptomycin. Mouse hepatocarcinoma cells H22, kindly supplied by Dr. Yuxin Li (National Laboratory for Gene and Protein in Drug Screening, Northeast Normal University, China), were maintained as described above. All the cells were incubated under standard culture condition (20% O_2 and 5% CO_2, 37 °C). TSA was purchased from Sigma, and sodium butyrate (NaB) was purchased from Bio Basic Inc. (BBI).

6.2.2. Plasmid construct

The WWP-Luc-1 construct (a gift from Dr. Vogelstein, Johns Hopkins University, Baltimore, MD) contains the 2.3-kb *Hind*III fragment of the *p21* gene promoter inserted into the pGL3-Enhancer vector (Promega). The recombinant fragment containing *p21* promoter and luciferase gene was produced by digesting with *Bgl*II and *Xba*I and inserting the 4.1-kb *Bgl*II-*Xba*I fragment into the *Sma*I- and *Hind*III-digested pCI-neo vector (Promega). The purified pCI-*p21*-luc-neo plasmid was used for transfection.

6.2.3. Construction of stably transfected cell line

HEK293 cells were transfected with pCI-*p21*-luc-neo plasmid using the calcium phosphate-mediated gene transfer method. Cells were maintained in IMDM medium supplemented with 10% FBS, 100 mg/mL penicillin, 100 mg/mL streptomycin and 1000 μg/mL G418. After 15–22 days, individual colonies were isolated and expanded. Stably transfected cell line was maintained in IMDM supplemented with 10% FBS in the presence of G418 (1000 μg/mL). The cell line was used for screening of potential HDAC inhibitors.

6.2.4. Screening of potential polyoxometalate HDACIs

The transfected cells were plated onto the 96-well plates at a density of 5000 cells/mL, and the plates were incubated for 24 h. Cells were treated with different types of polyoxometalate compounds at variable concentrations for 24 h, before they were incubated on plates for 15 min. The cell lysates were then subject to luciferase activity assay by using a Squal-luciferase reporter assay system (Promega) according to the manufacturer's instruction.

6.2.5. HDAC inhibition assay

The HDAC inhibition assay was performed using an HDAC fluorescent activity assay kit (BIOMOL, Inc.), following the manufacturer's recommendations. In brief, 5 μg of HeLa cell nuclear extract was added to the diluted HDAC inhibitor, and the substrate was added. Samples were incubated for 30 min at 25 °C, and the reaction was terminated by adding the developer. Fluorescence was analyzed on an LS55 luminescence spectrometer (Perkin–Elmer).

6.2.6. Cytotoxicity assay (MTT method)

Cells were seeded onto 96-well plates and incubated for 24 h at 37 °C before treated with drugs (PAC-320, TSA and NaB) for 3 days at 37 °C. After the treatments, 3-(4,5-dimethylthiazol-2-yl)-2,5-diphenyltetrazolium bromide solution was added to each well and incubated for 4 h at 37 °C before removal of the culture medium. DMSO was then added and shaken for 30 min at room temperature. Cell viability was determined by measuring the absorbance at 492 nm. Values represent the mean of 3 experiments (bars, ±SD).

6.2.7. Immunoblotting analysis

Cells were seeded onto 6-well plates and incubated for 24 h at 37 °C before treated with drugs (PAC-320, and NaB) for 24 h at 37 °C. After the treatments, cells were harvested and lysed in the lysis buffer (50 mM Tris–HCl, 1% Nonidet P-40, 150 mM NaCl, 1 mM EDTA, and 1 mM phenylmethanesulfonyl fluoride) for 30 min on ice. Total cell extracts were separated in 12% SDS-polyacrylamide gel electrophoresis (PAGE), and then transferred to a polyvinylidene fluoride membrane (Millipore, Bedford, MA, USA). The membranes were incubated with anti-acetylated-H3 (Upstate Biotechnology, NY), or anti-β-actin (Sigma) antibodies. The signals were visualized by using the Chemiluminescent Substrate method using the SuperSignal West Pico kit provided by Pierce Co (Rockford, IL, USA).

6.2.8. Determination of in vivo antitumor activity

To test the antitumor activities of PAC-320 *in vivo*, mouse hepatocarcinoma H22 cells were transplanted s.c. into the right subaxillary region of mice. Mice bearing the tumor were randomized into "treated" and "control" groups of 6 mice per group. Four days after inoculation, compounds (PAC-320, CTK) were administered i.p. per day for 14 days at an indicated dose (determined previously as the maximum tolerated dose). Tumors were measured using a Vernier caliper, and tumor volume (V) was calculated daily using the equation $V = 1/2ab^2$, where a and b represent the length and width, respectively (in millimeters).

6.2.9. Statistical analysis

The Student's *t*-test was used to calculate the statistical significance of the experimental data. The significance level was set as $^*P$, $P < 0.05$; $^{**}P$, $P < 0.01$.

Acknowledgments

We gratefully acknowledge the financial supports to this work from The National Basic Research Program of China (2006CB910506), The Science and Technology Office of Jilin Province (20075021), The National Science Foundation of China (20871027), The Program for Changjiang Scholars Innovative Research Team (PCSIRT) in Universities (IRT0519), and The Program for New Century Excellent Talents in Universities (NCET-07-0169).

Appendix. Supplementary material

The supplementary data associated with this article can be found in the on-line version at doi:10.1016/j.ejmech.2011.03.036.

References

[1] J.R. Davie, D.N. Chadee, J. Cell Biochem.(Suppl. 30–31) (1998) 203–213.
[2] T. Kouzarides, Curr. Opin. Genet. Dev. 9 (1999) 40–48.
[3] H.R. Kim, E.J. Kim, S.H. Yang, E.T. Jeong, C. Park, J.H. Lee, M.J. Youn, H.S. So, R. Park, Exp. Mol. Med. 38 (2006) 616–624.
[4] N. Takai, J.C. Desmond, T. Kumagai, D. Gui, J.W. Said, S. Whittaker, I. Miyakawa, H.P. Koeffler, Clin. Cancer Res. 10 (2004) 1141–1149.
[5] Y. Yamashita, M. Shimada, N. Harimoto, T. Rikimaru, K. Shirabe, S. Tanaka, K. Sugimachi, Int. J. Cancer 103 (2003) 572–576.
[6] J.W. Harper, G.R. Adami, N. Wei, K. Keyomarsi, S.J. Elledge, Cell 75 (1993) 805–816.
[7] S. Waga, G.J. Hannon, D. Beach, B. Stillman, Nature 369 (1994) 574–578.
[8] Y. Sowa, T. Orita, S. Hiranabe-Minamikawa, K. Nakano, T. Mizuno, H. Nomura, T. Sakai, Ann. N. Y. Acad. Sci. 886 (1999) 195–199.
[9] Y. Sowa, T. Orita, S. Minamikawa-Hiranabe, T. Mizuno, H. Nomura, T. Sakai, Cancer Res. 59 (1999) 4266–4270.
[10] W. Huang, D. Tan, X. Wang, S. Han, J. Tan, Y. Zhao, J. Lu, B. Huang, Biochem. Biophys. Res. Commun. 339 (2006) 165–171.
[11] G. Lagger, A. Doetzlhofer, B. Schuettengruber, E. Haidweger, E. Simboeck, J. Tischler, S. Chiocca, G. Suske, H. Rotheneder, E. Wintersberger, C. Seiser, Mol. Cell Biol. 23 (2003) 2669–2679.
[12] D. Mottet, S. Pirotte, V. Lamour, M. Hagedorn, S. Javerzat, A. Bikfalvi, A. Bellahcene, E. Verdin, V. Castronovo, Oncogene 28 (2009) 243–256.

[13] J.J. Westendorf, S.K. Zaidi, J.E. Cascino, R. Kahler, A.J. van Wijnen, J.B. Lian, M. Yoshida, G.S. Stein, X. Li, Mol. Cell. Biol. 22 (2002) 7982–7992.
[14] A.J. Wilson, D.S. Byun, N. Popova, L.B. Murray, K. L'Italien, Y. Sowa, D. Arango, A. Velcich, L.H. Augenlicht, J.M. Mariadason, J. Biol. Chem. 281 (2006) 13548–13558.
[15] C.Y. Gui, L. Ngo, W.S. Xu, V.M. Richon, P.A. Marks, Proc. Natl. Acad. Sci. U S A 101 (2004) 1241–1246.
[16] L. Huang, Y. Sowa, T. Sakai, A.B. Pardee, Oncogene 19 (2000) 5712–5719.
[17] K.B. Glaser, Biochem. Pharmacol. 74 (2007) 659–671.
[18] S. Minucci, P.G. Pelicci, Nat. Rev. Cancer 6 (2006) 38–51.
[19] L.N. Pan, J. Lu, B. Huang, Cell. Mol. Immunol. 4 (2007) 337–343.
[20] P.A. Marks, Oncogene 26 (2007) 1351–1356.
[21] D.A. Judd, J.H. Nettles, N. Nevins, J.P. Snyder, D.C. Liotta, J. Tang, J. Ermolieff, R.F. Schinazi, C.L. Hill, J. Am. Chem. Soc. 123 (2001) 886–897.
[22] C.Y. Sun, S.X. Liu, D.D. Liang, K.Z. Shao, Y.H. Ren, Z.M. Su, J. Am. Chem. Soc. 131 (2009) 1883–1888.
[23] D.L. Long, R. Tsunashima, L. Cronin, Angew. Chem. Int. Ed. Engl. 49 (2010) 1736–1758.
[24] J.T. Rhule, C.L. Hill, D.A. Judd, R.F. Schinazi, Chem. Rev. 98 (1998) 327–358.
[25] I.S. Lee, J.R. Long, S.B. Prusiner, J.G. Safar, J. Am. Chem. Soc. 127 (2005) 13802–13803.
[26] Q. Wu, J. Wang, L. Zhang, A. Hong, J. Ren, Angew. Chem. Int. Ed. Engl. 44 (2005) 4048–4052.
[27] T. Yamase, J. Mater. Chem. (2005) 4773–4782.
[28] S. Mitsui, A. Ogata, H. Yanagie, H. Kasano, T. Hisa, T. Yamase, M. Eriguchi, Biomed. Pharmacother. 60 (2006) 353–358.
[29] A. Ogata, S. Mitsui, H. Yanagie, H. Kasano, T. Hisa, T. Yamase, M. Eriguchi, Biomed. Pharmacother. 59 (2005) 240–244.
[30] H. Thomadaki, A. Karaliota, C. Litos, A. Scorilas, J. Med. Chem. 50 (2007) 1316–1321.
[31] X.H. Wang, J.F. Liu, Y.G. Chen, L. Meng, J. Chem. Soc. Dalton Trans. 7 (2000) 1139–1141.
[32] T. Yamase, Mol. Eng. 3 (1993) 241–262.
[33] R. Prudent, V. Moucadel, B. Laudet, C. Barette, L. Lafanechere, B. Hasenknopf, J. Li, S. Bareyt, E. Lacote, S. Thorimbert, M. Malacria, P. Gouzerh, C. Cochet, Chem. Biol. 15 (2008) 683–692.
[34] C.E. Müller, J. Iqbal, Y. Baqi, H. Zimmermann, A. Rollich, H. Stephan, Bioorg. Med. Chem. Lett. 16 (2006) 5943–5947.
[35] B. Heltweg, M. Jung, Anal. Biochem. 302 (2002) 175–183.
[36] K. Hoffmann, G. Brosch, P. Loidl, M. Jung, Nucleic Acids Res. 27 (1999) 2057–2058.
[37] B. Nare, J.J. Allocco, R. Kuningas, S. Galuska, R.W. Myers, M.A. Bednarek, D.M. Schmatz, Anal. Biochem. 267 (1999) 390–396.
[38] D. Wegener, F. Wirsching, D. Riester, A. Schwienhorst, Chem. Biol. 10 (2003) 61–68.
[39] C.L. Wang, S.X. Liu, C.Y. Sun, L.H. Xie, Y.H. Ren, D.D. Liang, H.Y. Cheng, J. Mol. Struct. 841 (2007) 88–95.
[40] Z.M. Zhang, E.B. Wang, Y. Li, H.Y. An, Y. Qi, L. Xu, J. Mol. Struct 872 (2008) 176–181.
[41] Y.H. Ren, S.X. Liu, R.G. Cao, X.Y. Zhao, J.F. Cao, C.Y. Gao, Inorg. Chem. Commun. 11 (2008) 1320–1322.
[42] F. Xin, M.T. Pope, Organometallics 13 (12) (1994) 4881–4886.
[43] H. Fujita, T. Fujita, T. Sakurai, T. Yamase, Y. Seto, Tohoku J. Exp. Med. 168 (1992) 421–426.
[44] M. Sadakane, E. Steckhan, Chem. Rev. 98 (1998) 219–238.
[45] R. Feng, H. Ma, C.A. Hassig, J.E. Payne, N.D. Smith, M.Y. Mapara, J.H. Hager, S. Lentzsch, Mol. Cancer Ther. 7 (2008) 1494–1505.
[46] S.K. Kulp, C.S. Chen, D.S. Wang, C.Y. Chen, Clin. Cancer Res. 12 (2006) 5199–5206.
[47] J.H. Park, Y. Jung, T.Y. Kim, S.G. Kim, H.S. Jong, J.W. Lee, D.K. Kim, J.S. Lee, N.K. Kim, Y.J. Bang, Clin. Cancer Res. 10 (2004) 5271–5281.
[48] S.J. Li, S.X. Liu, C.C. Li, F.J. Ma, D.D. Liang, W. Zhang, R.K. Tan, Y.Y. Zhang, L. Xu, Chem. Eur. J. 16 (2010) 13435–13442.